Impact of orthogonal optical feedback on the polarization switching of vertical-cavity surface-emitting lasers

Jon Paul,[1,*] Cristina Masoller,[2] Yanhua Hong,[1] Paul S. Spencer,[1] and K. Alan Shore[1]

[1]*School of Electronics, University of Wales, Bangor, Dean Street, Bangor LL57 1UT, Wales, UK*
[2]*Departament de Fisica i Enginyeria Nuclear, Universitat Politecnica de Catalunya, Colom 11, E-08222 Terrassa, Spain*
[*]*Corresponding author: jpaul@informatics.bangor.ac.uk*

Received October 27, 2006; revised March 1, 2007; accepted April 12, 2007; posted May 1, 2007 (Doc. ID 76519); published July 19, 2007

We study experimentally and numerically the influence of orthogonal optical feedback on the polarization-resolved light versus bias current characteristic ($L–I$ curve) of vertical-cavity surface-emitting lasers (VCSELs). The feedback scheme is such that only one linear polarization is selected to be fed back into the laser while the orthogonal polarization is completely suppressed before the output is rotated 90° and reinjected into the laser. We experimentally demonstrate that weak feedback levels modify the polarization switching point only slightly, but as the feedback increases the otherwise depressed mode grows and the hysteresis is suppressed. While polarization-preserved and X-orthogonal feedback have similar effects (X indicates the direction of the polarization selected at threshold), Y-orthogonal feedback strongly modifies the shape of the $L–I$ curve, even suppressing the polarization-switching for strong enough feedback. Numerical simulations of the spin-flip model show good qualitative agreement with the observations. We also analyze the influence of various parameters, such as linear birefringence, dichroism, and the spin-flip relaxation rate.

OCIS codes: 250.7260, 260.5430.

1. INTRODUCTION

Vertical-cavity surface-emitting lasers (VCSELs) have many advantages compared with conventional edge-emitting semiconductor lasers. They have single-longitudinal-mode emission with a circular output profile, very low threshold currents, and can be integrated into large 2D arrays. However, because of their circular transverse geometry the orientation of the polarization of the emitted light is not fixed by geometrical constraints (as it is in edge-emitting lasers). Due to residual anisotropies that break the circular transverse symmetry, the output of a VCSEL is often linearly polarized along one of two orthogonal directions. When a VCSEL begins to lase one linear polarization dominates (which we refer to as X), and when the bias current is increased in many devices it is observed that the emission switches to the orthogonal linear polarization (which we refer to as Y). Such polarization switching (PS) is usually accompanied by complex polarization dynamics in which there is either polarization coexistence (simultaneous emission in both of the orthogonal linear polarizations with different emission frequencies), polarization hopping (noise-induced competition between the two orthogonal linear polarizations with different emission frequencies), or emission of elliptically polarized light (on both orthogonal linear polarizations with the same emission frequency). Polarization instabilities are detrimental for the use of VCSELs in polarization-sensitive applications, and a lot of effort has been devoted to understand the mechanisms that determine the polarization of the emitted light [1–8]. Methods to suppress polarization instabilities, such as the use of anisotropic post structures [9] or polarization-selective optical feedback [10,11], have been experimentally demonstrated. The effects of isotropic optical feedback on polarization switching of VCSELs have also been studied in detail [12–14].

On the other hand, exploiting the polarization degree of freedom of light can lead to new ways of transmitting secure information [15,16]. Synchronization of chaos was achieved experimentally [17] in unidirectionally coupled VCSELs, when the polarization of the transmitter is perpendicular to the polarization of the free-running receiver. The transmitter output and the Y-polarized receiver output showed identity (positive-slope) synchronization, while the transmitter output and the X-polarized receiver output showed inverse (negative-slope) synchronization. The possibility of message encoding and decoding using this synchronization scheme was also experimentally demonstrated [18]. Identity and inverse synchronization have also been found in conventional edge-emitting lasers [19], with a coupling scheme such that the transmitter and receiver lasers are subjected to orthogonal optical feedback and to orthogonal optical injection, respectively (the TE mode is reinjected into the TM mode).

Recent studies of the dynamics of diode lasers with orthogonal optical feedback have shown the potential for fast optical pulse generation [20,21]. It is well known that, by placing a quarter-wave-plate (QWP) in the external cavity, fast polarization self-modulation can be

achieved [22–24], which has interesting applications [25]. The orthogonal-feedback scheme differs from the QWP-feedback scheme because in the case of orthogonal feedback only one polarization (e.g., the X polarization) is selected to be fed back into the laser while the other polarization is completely suppressed before the output is rotated 90° and reinjected into the laser. Therefore, the orthogonal-feedback scheme couples the two polarizations unidirectionally ($X \rightarrow Y$ or $Y \rightarrow X$) while the QWP-feedback scheme couples them bidirectionally ($X \rightarrow Y$ and $Y \rightarrow X$). The orthogonal-feedback scheme was recently proposed theoretically as a novel approach for inducing passive mode locking without using any saturable absorber [26]. In this approach gain modulation is caused by the delayed reinjection of the polarization-rotated laser output. The delay time defines resonance tongues that correspond to mode-locking operation. For VCSELs the analysis predicts stable mode-locked pulses at repetition rates in the gigahertz range with pulse widths of few tens of picoseconds.

In this paper we study experimentally and numerically the influence of orthogonal optical feedback on the polarization-resolved light versus bias current characteristic ($L-I$ curve) of VCSELs. We find that weak feedback levels only slightly modify the PS point, but as the feedback increases the otherwise depressed mode grows and the hysteresis is suppressed. While polarization-preserved and X-orthogonal feedback have similar effects, Y-orthogonal feedback strongly modifies the shape of the $L-I$ curve, even suppressing the PS for strong enough feedback (we recall that X indicates the direction of the polarization selected at threshold). We show that numerical simulations using the spin-flip model [3] are in good qualitative agreement with the observations.

This paper is organized as follows. Section 2 presents the experimental measurements of the polarization-resolved $L-I$ curve under the influence of polarization-rotated feedback. For comparison, we also present measurements of the influence of polarization-preserved optical feedback. Section 3 presents results of numerical simulations based on the spin-flip model, that are in good qualitative agreement with the experiments. We also analyze the influence of various parameters. Section 4 presents a summary and the conclusions.

2. EXPERIMENTS

The experimental setup is similar to that employed in [21] and is shown in Fig. 1. A commercial single-

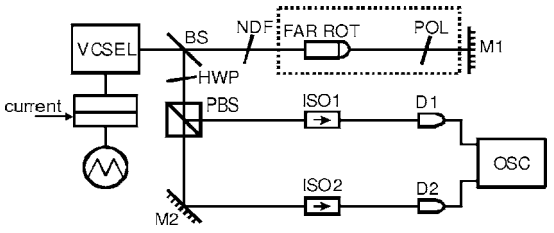

Fig. 1. Schematic of experimental setup arrangement. BS, beam splitter; NDF, neutral-density filter; FAR ROT, Faraday rotator; POL, polarizer; M1, M2, mirrors; HWP, half-wave plate; PBS, polarization beam splitter; ISO1, ISO2, optical isolators; D1, D2, photodetectors; OSC, oscilloscope.

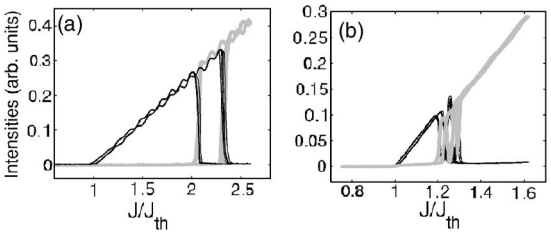

Fig. 2. Polarization-resolved $L-I$ curve. (a) First VCSEL. (b) Second VCSEL. The polarization selected at threshold (x) is indicated with a black curve, the orthogonal polarization (y) is indicated with a gray curve.

longitudinal-mode and single-transverse-mode VCSEL was driven by an ultra-low-noise current source and temperature controlled to within 0.01 K. The VCSEL output was collimated by using an anti-reflection-coated laser diode objective lens. The half-wave plate (HWP) and polarization beam splitter (PBS) were used to direct the two orthogonal linear polarizations to detectors D1 and D2. Two optical isolators (ISO1 and ISO2) with greater than −40 dB isolation were used to prevent light feedback from the detectors into the VCSEL. The output from the detectors were stored in a 1 GHz bandwidth digital oscilloscope (OSC). The OSC employed a low-pass filter to eliminate fast noisylike oscillations induced by the feedback. The laser threshold current is $J_{th}=2.65$ mA. The current supplied to the VCSEL was modulated by a 1 KHz triangular signal with a dc value of 3.59 mA and a modulation amplitude of 6.6 mA. The optical feedback to the VCSEL is provided by a Faraday rotator, a polarizer, and a mirror (M1) forming an external cavity of length 64 cm (giving a delay time of $\tau=4.6$ ns). The beam polarization is rotated 45° by the Faraday rotator (which is an optical isolator with the input polarizer removed). After emerging from the rotator, the beam passes through a polarizer and is then reflected by M1. After a second pass through the polarizer, the beam polarization is then rotated by another 45° by the Faraday rotator, thus providing 90° polarization rotated feedback. The use of a Faraday rotator prevents multiple cavity round trips of the laser beam. A neutral-density filter (NDF) controls the feedback strength.

Figure 2(a) displays the polarization-resolved $L-I$ curve of the free-running VCSEL. The VCSEL begins to lase with a polarization direction referred to as X (black curve). As the bias current increases, an abrupt PS to the orthogonal direction Y (gray curve) is observed at $J/J_{th} \sim 2.2$. When the bias current decreases, hysteresis is observed and the polarization switches back to the X direction at $J/J_{th} \sim 2$.

Figures 3–5 display the measured $L-I$ characteristic of the VCSEL under three different feedback conditions.

(i) The Y polarization is suppressed from the laser output, and the polarization direction of the reinjected light is rotated by 90°. In this way the X polarization is coupled unidirectionally to the Y polarization, $X \rightarrow Y$. We refer to this scheme as X-orthogonal feedback. Results are displayed in Fig. 3.

(ii) The X polarization is suppressed from the laser output, and the polarization direction of the reinjected

light is rotated by 90°. In this way the Y polarization is coupled unidirectionally to the X polarization, $Y \rightarrow X$. We refer to this scheme as Y-orthogonal feedback. Results are displayed in Fig. 4.

(iii) The optical feedback is isotropic and preserves the polarization of the emitted light (for these measurements the Faraday rotator and the polarizer, shown in the dashed-line box of Fig. 1, were removed). Results are displayed in Fig. 5.

For polarization-rotated feedback the feedback ratio is defined as the ratio of the feedback power (measured just before the light returns to the laser diode objective) to the output power in the selected polarization; for polarization-preserved feedback, the feedback ratio is defined as the ratio of the feedback power to the total VCSEL output power.

It can be observed that for weak feedback levels there is only a slight modification of the PS points and a reduction of the bistability region. As the feedback increases the otherwise depressed mode grows and the hysteresis is suppressed. X-orthogonal feedback leads to a gradual increase of the intensity of the Y polarization *before* the PS point, but it has almost no effect well above the PS point, where the X polarization is off and therefore the feedback has no effect. Y-orthogonal feedback leads to a gradual increase of the intensity of the X polarization *after* the PS point, but it has almost no effect before the PS point, because the Y polarization is off and therefore there is no feedback. While polarization-preserved and X-orthogonal feedback seem to have similar effects, Y-orthogonal feedback strongly modifies the shape of the L–I curve, even suppressing the PS for strong enough feedback. We think

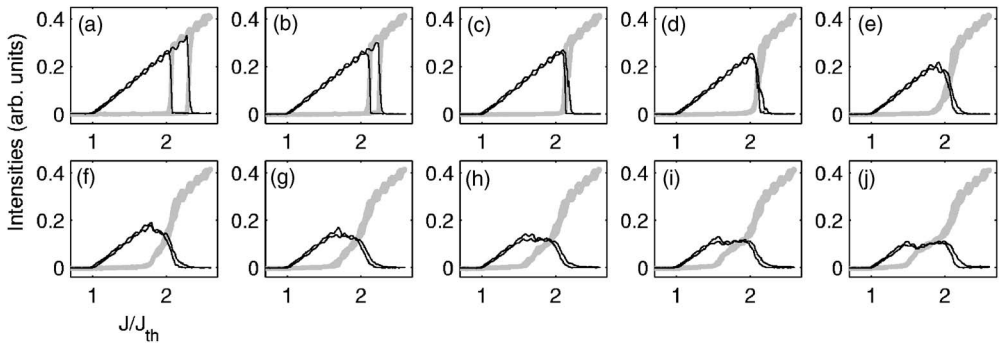

Fig. 3. Polarization-resolved L–I characteristic measured experimentally for the (a) free-running laser, (b)–(j) laser with X-orthogonal feedback. The polarization selected at threshold (X) is indicated with a black curve, the orthogonal polarization (Y) is indicated with a gray curve. The feedback ratios are −22, −19, −17.6, −15.4, −13.1, −12.2, −11, −9.9, and −9 dB, respectively.

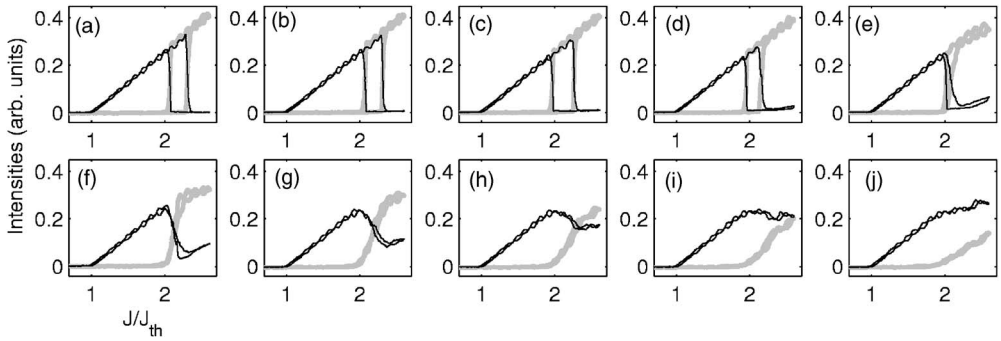

Fig. 4. Polarization-resolved L–I characteristic measured experimentally for the (a) free-running laser, (b)–(j) laser with Y-orthogonal feedback. The feedback ratios are −22, −19, −17.6, −15.4, −13.1, −12.2, −11, −9.9, and −9 dB, respectively.

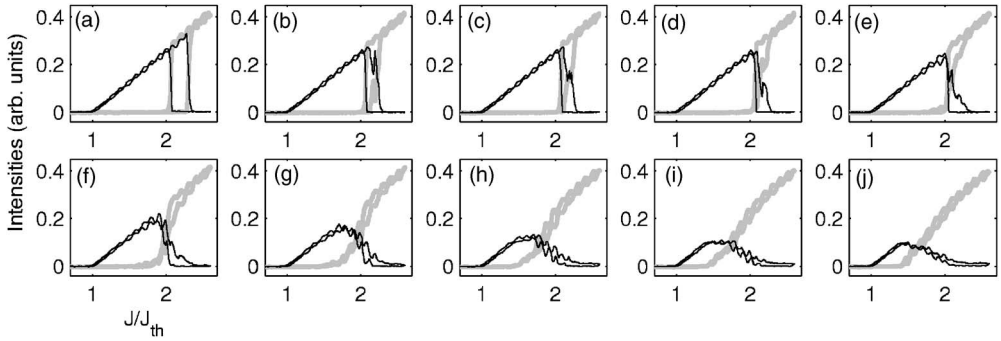

Fig. 5. Polarization-resolved L–I characteristic measured experimentally for the (a) free-running laser, (b)–(j) laser with polarization preserved feedback. The feedback ratios are −21, −18.6, −16.5, −14.3, −12.3, −11.1, −9.9, −8.9, and −7.9 dB, respectively.

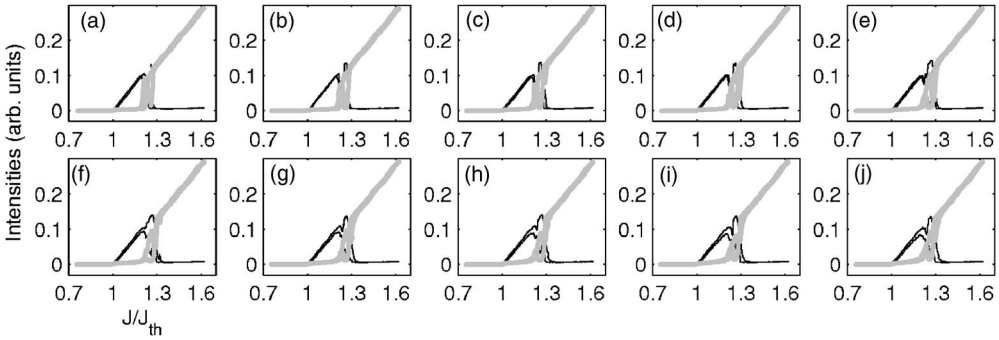

Fig. 6. Influence of X-orthogonal feedback on the second VCSEL device. (a) Free-running laser, (b)–(j) the feedback ratios are −22, −19, −17.6, −15.4, −13.1, −12.2, −11, −9.9, and −9 dB, respectively. The polarization selected at threshold (X) is indicated with a black curve, the orthogonal polarization (Y) is indicated with a gray curve.

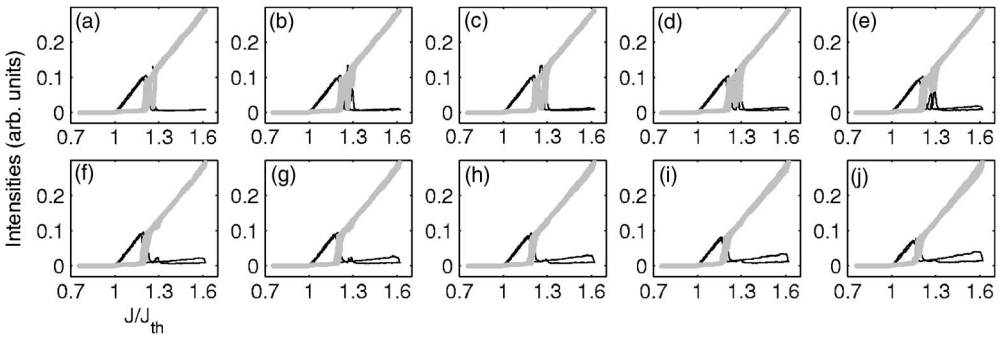

Fig. 7. Influence of Y-orthogonal feedback on the second VCSEL device. (a) Free-running laser, (b)–(j) the feedback ratios are −22, −19, −17.6, −15.4, −13.1, −12.2, −11, −9.9, and −9 dB, respectively.

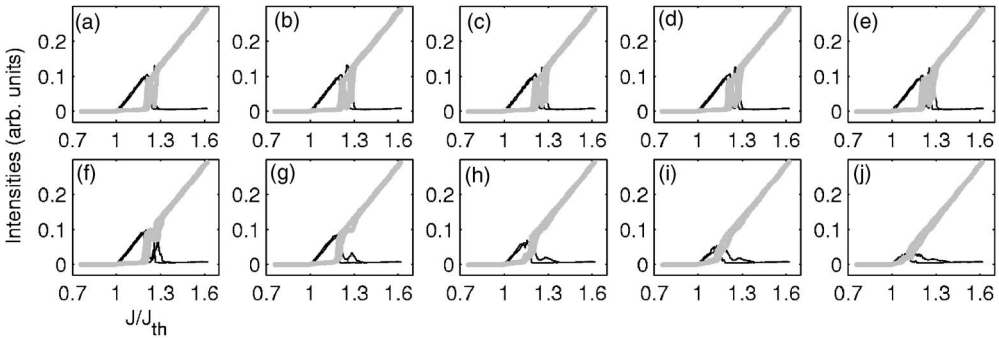

Fig. 8. Influence of polarization-preserved feedback on the second VCSEL device. (a) Free-running laser, (b)–(j) the feedback ratios are −21, −18.6, −16.5, −14.3, −12.3, −11.1, −9.9, −8.9, and −7.9 dB, respectively.

that this difference is due to the fact that Y-orthogonal feedback is effective above the PS point, where the laser output is stronger and thus, the feedback is stronger.

To investigate the generality of the above-presented results, we also performed experiments using a second VCSEL device that, under free-running conditions, exhibits a complex polarization-switching dynamics, shown in Fig. 2(b). The influence of orthogonal and polarization-preserved feedback in the L–I curve is displayed in Figs. 6–8. It can be observed that the effect of feedback is qualitatively the same as before (reducing the bistability region and turning on the otherwise depressed orthogonal mode), but in this laser the feedback has less impact. With X-orthogonal feedback we observe a small increase of the intensity of the Y-polarization before the PS, while with Y-orthogonal feedback we observe a small increase of the intensity of the X-polarization after the PS. We speculate that the smaller impact of feedback in this second VCSEL is because the internal anisotropies determining light polarization are stronger and/or the facet reflectivies are larger, diminishing the feedback sensitivity.

3. THEORY

In this section we present results of simulations of the spin-flip model [3] that are in good agreement with the observations. The rate equations for the linearly polarized slowly varying complex amplitudes, E_x and E_y; the total carrier density, $N=N_+ + N_-$; and the carrier difference, $n = N_+ - N_-$ (where N_+ and N_- are two carrier populations with positive and negative spin value) are [3]

$$\dot{E}_{x,y} = k(1+j\alpha)[(N-1)E_{x,y} \pm jnE_{y,x}] \mp (\gamma_a + j\gamma_p)E_{x,y} + \sqrt{\beta_{sp}}\xi_{x,y} + \eta_{x,y}E_{y,x}(t-\tau)e^{-i\omega\tau} + \eta E_{x,y}(t-\tau)e^{-i\omega\tau}, \quad (1)$$

$$\dot{N} = \gamma_N[\mu - N(1+|E_x|^2+|E_y|^2) + jn(E_yE_x^* - E_xE_y^*)], \quad (2)$$

$$\dot{n} = -\gamma_s n - \gamma_N[n(|E_x|^2+|E_y|^2) + jN(E_yE_x^* - E_xE_y^*)]. \quad (3)$$

Here k is the field decay rate, γ_N is the decay rate of the total carrier population, γ_s is the spin-flip rate, and α is the linewidth enhancement factor. γ_a and γ_p are linear anisotropies representing dichroism and birefringence, respectively, [3]. γ_a leads to different gain-to-loss ratios and therefore to different thresholds for the two polarizations, with the y polarization having the lower threshold when γ_a is positive. γ_p leads to a frequency split between the two polarizations, with the x polarization having the lower frequency when γ_p is positive. β_{sp} is the strength of the spontaneous emission noise and $\xi_{x,y}$ are independent Gaussian white-noise sources with zero mean and unit variance. $\mu = J/J_{th}$ where J is the injection current and J_{th} is the threshold current.

The last two terms in Eq. (1) represent the effect of optical feedback. τ is the delay time and ω is the reference frequency, which is the average between the frequencies of the two polarizations, $\omega = (\omega_x + \omega_y)/2$. The coefficients η_x, η_y, and η allow to model the above-discussed orthogonal and polarization-preserved feedback schemes, if they are chosen as

(i) x-orthogonal feedback: the y polarization is suppressed and the x polarization is rotated 90° and then is reinjected into the laser ($x \rightarrow y$). The feedback strengths are $\eta = \eta_x = 0$, $\eta_y \neq 0$.

(ii) y-orthogonal feedback: the x polarization is suppressed and the y polarization is rotated 90° and then is reinjected into the laser ($y \rightarrow x$). The feedback strengths are $\eta = \eta_y = 0$, $\eta_x \neq 0$.

(iii) Isotropic, polarization-preserved feedback: $\eta_x = \eta_y = 0$, $\eta \neq 0$.

We consider a linear variation of the emission wavelengths $\lambda_{x,y}$ with the injected current μ:

$$\lambda_{x,y} = \lambda_{x,y,th} + AJ_{th}(\mu - 1), \quad (4)$$

where A is a constant coefficient. Equation (4) incorporates the main effect of joule heating in semiconductor devices: a change in the background refractive index and hence a shift in the cavity resonances.

In the absence of feedback the solutions of the model are either two orthogonal linear polarized states ($|E_x|^2 = \mu - 1$, $|E_y|^2 = 0$ and $|E_x|^2 = 0$, $|E_y|^2 = \mu - 1$) or elliptically polarized states. Their stability is determined by the net gain-to-loss ratio, the birefringence, and the saturable dispersion of the material. For certain parameters the model predicts a PS due to a change of stability of the solutions for increasing injection current [3].

We solved numerically the model equations with typical VCSEL parameters: $k = 300\ \text{ns}^{-1}$, $\alpha = 3$, $\gamma_n = 1\ \text{ns}^{-1}$, $\beta_{sp} = 10^{-6}\ \text{ns}^{-1}$, $\tau = 4.6$ ns, and $A = 0.47$ nm/mA. First, we present results of simulations for parameters that correspond to the first VCSEL device used in the experiments, and show that the model gives a good agreement with the observations. In a second step, we discuss different feedback scenarios by studying the influence of various parameters.

To model the experimental situation, the parameters γ_a, γ_p, and γ_s were adjusted such that (i) the frequency split between the two polarizations and (ii) the hysteresis region of the free-running laser correspond to those measured experimentally. In the experiments the PS occurs, for increasing injection current, from the high-frequency to the low-frequency polarization (type-I PS [5]), and the frequency split between the two modes is ~20 GHz. Therefore, the parameters used for the simulations are chosen such that γ_p and γ_a are positive, and the high-frequency polarization (y) turns on at threshold. For the parameters $\gamma_p = 70$ rad/ns, $\gamma_a = 3.3\ \text{ns}^{-1}$, and $\gamma_s = 30\ \text{ns}^{-1}$ the free-running laser shows a PS for up scans at $\mu \sim 2.2$, and for down scans, at $\mu \sim 2$.

Figures 9–11 display the numerically calculated L–I curve for these parameters and various feedback conditions: x-orthogonal feedback (Fig. 9), y-orthogonal feedback (Fig. 10), and polarization preserved feedback (Fig. 11). A 2.5 MHz bandwidth low-pass filter was applied to the time series of the polarization intensities, to simulate the filter used in the experiments. This filter eliminates the fast oscillations of the instantaneous intensities that,

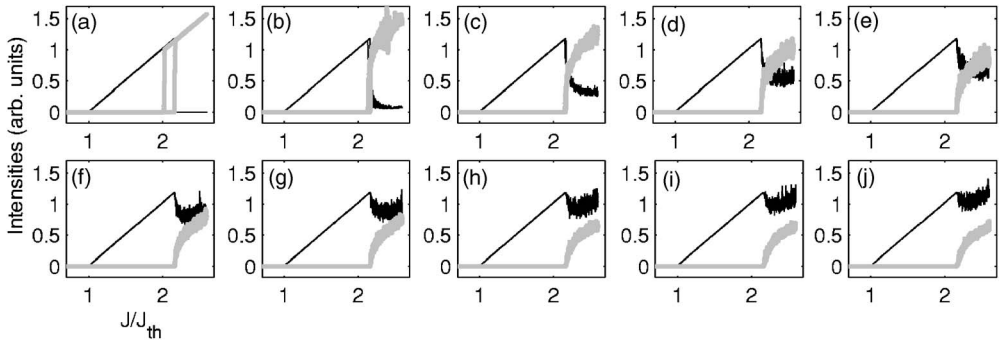

Fig. 9. Influence of x-orthogonal feedback, for parameters describing the first VCSEL device used in the experiments: $\gamma_p = 70$ rad/ns, other parameters as explained in the text. (a) Free-running laser. (b)–(j) η_y^2 increases linearly as $\eta_y^2 = a\,\eta_m^2$, with $\eta_m = 70$ GHz and a = (a) 0.1 to (j) 1.0. The polarization selected at threshold (y) is indicated with a black curve, the orthogonal polarization (x) is indicated with a gray curve.

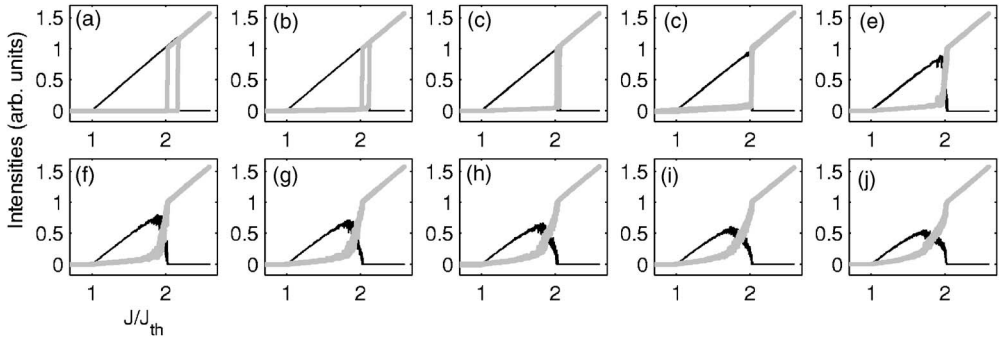

Fig. 10. Influence of y-orthogonal feedback. (a) Free-running laser. (b)–(j) η_x^2 increases linearly: $\eta_x^2 = a\,\eta_m^2$, with $\eta_m = 70$ GHz and $a =$ (a) 0.1 to (j) 1.0. Other parameters are as in Fig. 9.

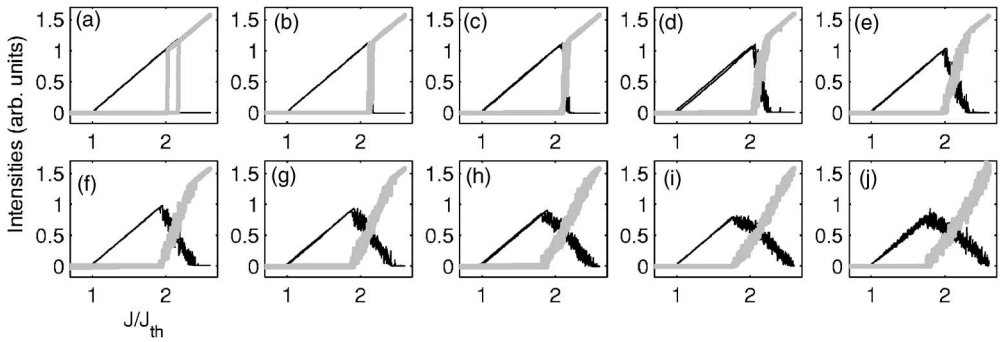

Fig. 11. Influence of polarization-preserved feedback. (a) Free-running laser. (b)–(j) η^2 increases linearly: $\eta^2 = a\,\eta_m^2$ with $\eta_m = 7$ GHz and $a =$ (a) 0.1 to (j) 1.0. Other parameters are as in Fig. 9.

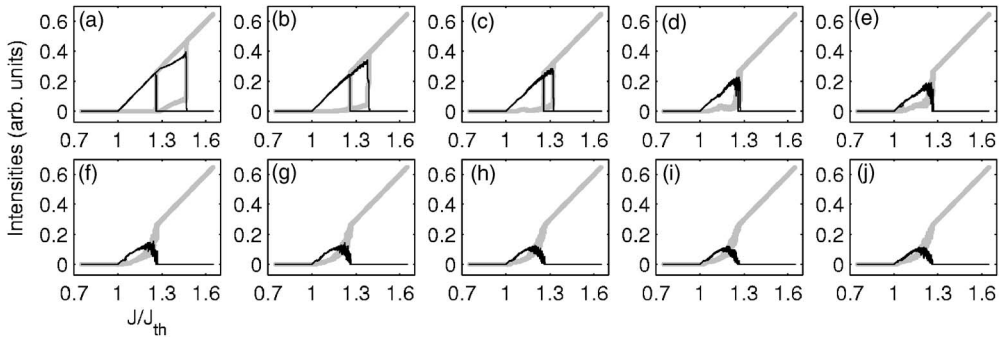

Fig. 12. Influence of x-orthogonal feedback for parameters corresponding to type-II PS. $\gamma_p = 5$ rad/ns, $\gamma_a = -0.3\ \mathrm{ns}^{-1}$, and $\gamma_s = 50\ \mathrm{ns}^{-1}$; other parameters as described in the text. (a) Free-running laser. (b)–(j) η_y^2 increases linearly: $\eta_y^2 = a\,\eta_m^2$ with $\eta_m = 5$ GHz and $a =$ from (a) 0.1 to (j) 1.0. The polarization selected at threshold (x) is indicated with a black curve, the orthogonal polarization (y) is indicated with a gray curve.

for strong enough feedback, seem chaotic and suggest a complex polarization dynamics that motivates future work.

When comparing the results of the simulations with the experimental observations, we have to take into account that in Figs. 3–5 X indicates the direction of the polarization selected at threshold. Therefore, the Y polarization in the simulations (the polarization with the highest frequency) corresponds to the X polarization in the experiments and Figs. 9 and 10 should be compared with Figs. 4 and 3, respectively. This comparison shows good qualitative agreement with the observations.

We have done extensive simulations and found that this scenario is robust and occurs for other values of γ_a, γ_s, and γ_p, as long as $\gamma_a > 0$ and $\gamma_p > \gamma_s/2\alpha$. If $\gamma_a < 0$ there is a different type of PS, which is analyzed below, while if $\gamma_p < \gamma_s/2\alpha$ the free-running laser does not present polarization switching: the y polarization is stable over the entire range of injection current. The influence of orthogonal feedback is qualitatively the same; however, the specific values of the feedback strengths vary: the larger is the frequency split between the two polarizations, the larger is the feedback strength needed to perturb the orthogonal mode.

So far we studied the PS that occurs from the high-frequency to the low-frequency polarization (known as type-I PS [5]). Next, we investigate type-II PS, which occurs from the low-frequency to the high-frequency polarization. For increasing current this PS occurs if $\gamma_a < 0$ (which gives the x polarization a lower threshold) and the

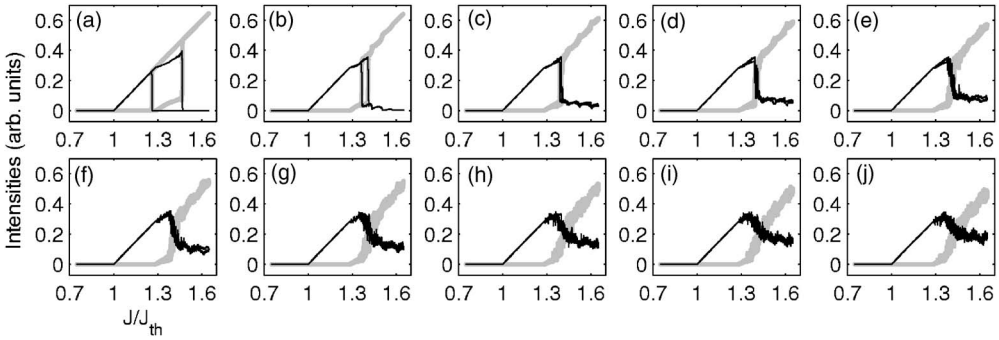

Fig. 13. Influence of y-orthogonal feedback for parameters corresponding to type-II PS. (a) Free-running laser. (b)–(j) η_x^2 increases linearly: $\eta_x^2 = a\,\eta_m^2$ with $\eta_m = 5$ GHz and $a =$ (a) 0.1 to (j) 1.0. Other parameters are as in Fig. 12.

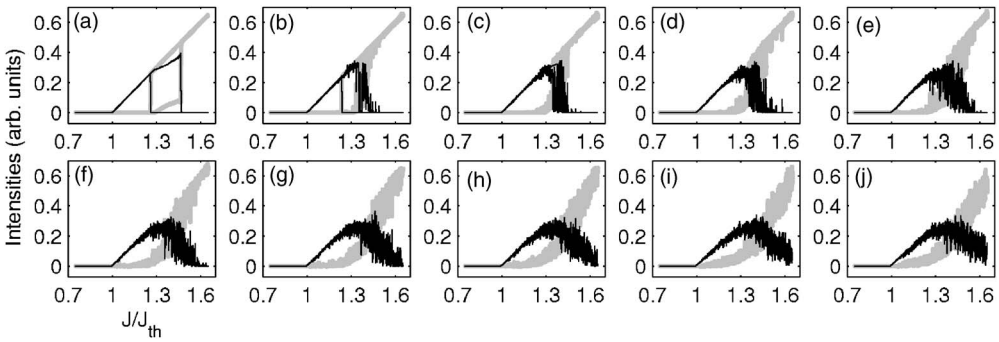

Fig. 14. Influence of polarization-preserved feedback for parameters corresponding to type-II PS. (a) Free-running laser. (b)–(j) η^2 increases linearly: $\eta^2 = a\,\eta_m^2$ with $\eta_m = 3$ GHz and $a =$ (a) 0.1 to (j) 1.0. Other parameters are as in Fig. 12.

birefringence is low (if $\gamma_p < \gamma_s/2\alpha$; for larger γ_p the x polarization is stable over the entire range of injection current). Type-II PS, which involves the destabilization of the polarization with the higher gain to loss ratio in favor of the weaker polarization, has been understood in terms of the interplay of birefringence, saturable dispersion, and spin-flip processes [3], and it usually involves the appearance of elliptically polarized states. Results are displayed in Figs. 12–14. We observe that, in spite of these differences, the influence of orthogonal feedback is qualitatively the same as type I. The feedback strengths needed to perturb the orthogonal polarization are now lower because the internal anisotropies (γ_a and γ_p) are weaker.

We also note that in both types of PS, with the orthogonal-feedback scheme larger feedback levels are required in order to perturb the laser emission, as compared with the isotropic feedback case [notice, e.g., that in Figs. 10(j) and 11(j) the feedback strengths are 70 and 7 ns^{-1}, respectively]. Due to coherent coupling with the lasing mode, in the case of isotropic feedback very low feedback levels are enough to drastically change the laser emission characteristics. On the contrary, the orthogonal feedback is coupled to the depressed mode, which does not lase in the absence of feedback, and thus, stronger feedback levels are required in order to overcome the losses and force this mode to start lasing.

4. CONCLUSIONS

Summarizing, we have studied experimentally and numerically the polarization switching of VCSELs in the presence of orthogonal optical feedback. We observed experimentally that weak feedback levels only slightly modify the PS point, but as the feedback increases the otherwise depressed mode grows and the hysteresis is suppressed. While polarization-preserved and X-orthogonal feedback have similar effects, Y-orthogonal feedback strongly modifies the shape of the L–I curve, even suppressing the PS for strong enough feedback. Simulations based on the spin-flip model are in good qualitative agreement with the experimental observations. We assumed fundamental transverse mode operation on the two orthogonal polarizations and neglected transverse effects such as spatial-hole-burning and carrier diffusion. The thermal shift of the gain curve with increasing bias current was also not taken into account. Nevertheless, the model includes key features determining the polarization of the light emitted by VCSELs: birefringence, gain or loss anisotropies, saturable dispersion, and an intermediate spin-flip relaxation rate. We have shown that these features provide a good qualitative understanding of the impact of orthogonal feedback. Our results provide experimental and theoretical insight into the dynamics of VCSELs with polarization-rotated feedback, which have been shown to have promising applications for high-frequency pulse generation, as well as for generating broadband chaotic dynamics suitable to be employed in secure optical communications.

In terms of future work, it is known that VCSELs present different types of polarization behaviors. While some devices do not present polarization switching at all, i.e., exhibit stable polarization emission in the whole range of injection currents, others switch more than once;

and, specifically, it has been previously found, both theoretically and experimentally [12–14,27], that some VCSELs, when subjected to isotropic optical feedback, undergo successive polarization switchings for increasing injection current. This so-called channeled behavior has been interpreted in terms of two polarizations that compete equally (with very close gain-to-loss ratios). In this situation, external optical feedback, depending on the feedback phase, can benefit one polarization more than the other one. As the feedback phase changes with the injection current (because the optical frequencies are bias-current dependent due to thermal effects), the feedback influence changes with the injection, leading to multiple switchings. This situation is expected to occur when anisotropies (dichroism and birefringence) are weak, and we speculate that it can also be found, under suitable conditions, with orthogonal feedback.

ACKNOWLEDGMENTS

J. Paul and Y. Hong acknowledge support from Engineering and Physical Sciences Research Council (UK) grants EP/C010612/1 and GR/S22936/01, C. Masoller acknowledges support from the Generalitat de Catalunya, through program AGAUR BE2006–00007, and from the Spanish Ministerio de Educación y Ciencia, through the program "Ramon y Cajal" and project FIS2005-07931-C03-03.

REFERENCES

1. Z. G. Pan, S. J. Jiang, M. Dagenais, R. A. Morgan, K. Kojima, M. T. Asom, R. E. Leibenguth, G. D. Guth, and M. W. Focht, "Optical-injection induced polarization bistability in vertical-cavity surface-emitting lasers," Appl. Phys. Lett. **63**, 2999–3001 (1993).
2. K. D. Choquette, R. P. Schneider, K. L. Lear, and R. E. Leibenguth, "Gain-dependent polarization properties of vertical-cavity lasers," IEEE J. Sel. Top. Quantum Electron. **1**, 661–666 (1995).
3. J. Martin-Regalado, F. Prati, M. San Miguel, and N. B. Abraham, "Polarization properties of vertical-cavity surface-emitting lasers," IEEE J. Quantum Electron. **33**, 765–783 (1997).
4. A. Valle, L. Pesquera, and K. A. Shore, "Polarization behavior of birefringent multitransverse mode vertical-cavity surface-emitting lasers," IEEE Photon. Technol. Lett. **9**, 557–559 (1997).
5. B. Ryvkin, K. Panajotov, A. Georgievski, J. Danckaert, M. Peeters, G. Verschaffelt, H. Thienpont, and I. Veretennicoff, "Effect of photon-energy-dependent loss and gain mechanisms on polarization switching in vertical-cavity surface-emitting lasers," J. Opt. Soc. Am. B **16**, 2106–2113 (1999).
6. S. Balle, E. Tolkachova, M. San Miguel, J. R. Tredicce, J. Martin-Regalado, and A. Gahl, "Mechanisms of polarization switching in single-transverse-mode vertical-cavity surface-emitting lasers: thermal shift and nonlinear semiconductor dynamics," Opt. Lett. **24**, 1121–1123 (1999)
7. T. Ackemann and M. Sondermann, "Characteristics of polarization switching from the low to the high frequency mode in vertical-cavity surface-emitting lasers," Appl. Phys. Lett. **78**, 3574–3576 (2001).
8. J. Paul, C. Masoller, Y. Hong, P. S. Spencer, and K. A. Shore, "Experimental study of polarization switching of vertical-cavity surface-emitting lasers as a dynamical bifurcation," Opt. Lett. **31**, 748–750 (2006).
9. T. Yoshikawa, T. Kawakami, H. Saito, H. Kosaka, M. Kajita, K. Kurihara, Y. Sugimoto, and K. Kasahara, "Polarization-controlled single-mode VCSEL," IEEE J. Quantum Electron. **34**, 1009–1015 (1998).
10. T. H. Russell and T. D. Milster, "Polarization switching control in VCSELs," Appl. Phys. Lett. **70**, 2520–2522 (1997).
11. Y. Hong, P. S. Spencer, and K. A. Shore, "Suppression of polarization switching in vertical-cavity surface-emitting lasers by use of optical feedback," Opt. Lett. **29**, 2151–2153 (2004).
12. A. Valle, L. Pesquera, and K. A. Shore, "Polarization selection and sensitivity of external cavity vertical-cavity surface-emitting laser diodes," IEEE Photon. Technol. Lett. **10**, 639–641 (1998).
13. P. Besnard, M. L. Chares, G. Stephan, and F. Robert, "Switching between polarized modes of a vertical-cavity surface-emitting laser by isotropic optical feedback," J. Opt. Soc. Am. B **16**, 1059–1063 (1999).
14. M. Sciamanna, K. Panajotov, H. Thienpont, I. Veretennicoff, P. Megret, and M. Blondel, "Optical feedback induces polarization mode hopping in vertical-cavity surface-emitting lasers," Opt. Lett. **28**, 1543–1545 (2003).
15. G. D. VanWiggeren and R. Roy, "Communication with dynamically fluctuating states of light polarization," Phys. Rev. Lett. **88**, 097903 (2002).
16. A. Scire, J. Mulet, C. R. Mirasso, J. Danckaert, and M. San Miguel, "Polarization message encoding through vectorial chaos synchronization in vertical-cavity surface-emitting lasers," Phys. Rev. Lett. **90**, 113901 (2003).
17. Y. Hong, M. W. Lee, P. S. Spencer, and K. A. Shore, "Synchronization of chaos in unidirectionally coupled vertical-cavity surface-emitting semiconductor lasers," Opt. Lett. **29**, 1215–1217 (2004).
18. M. W. Lee, Y. Hong, and K. A. Shore, "Experimental demonstration of VCSEL-based chaotic optical communications," IEEE Photon. Technol. Lett. **16**, 2392–2394 (2004).
19. D. W. Sukow, A. Gavrielides, T. McLachlan, G. Burner, J. Amonette, and J. Miller, "Identity synchronization in diode lasers with unidirectional feedback and injection of rotated optical fields," Phys. Rev. A **74**, 023812 (2006).
20. R. Ju and P. S. Spencer, "Dynamic regimes in semiconductor lasers subject to incoherent optical feedback," J. Lightwave Technol. **23**, 2513–2523 (2005).
21. A. Gavrielides, T. Erneux, D. W. Sukow, G. Burner, T. McLachlan, J. Miller, and J. Amonette, "Square-wave self-modulation in diode lasers with polarization-rotated optical feedback," Opt. Lett. **31**, 2006–2008 (2006).
22. S. J. Jiang, Z. Q. Pan, M. Dagenais, R. A. Morgan, and K. Kojima, "High-frequency polarization self-modulation in vertical-cavity surface-emitting lasers," Appl. Phys. Lett. **63**, 3545–3547 (1993).
23. H. Li, A. Hohl, A. Gavrielides, H. Hou, and K. D. Choquette, "Stable polarization self-modulation in vertical-cavity surface-emitting lasers," Appl. Phys. Lett. **72**, 2355–2357 (1998).
24. M. Sciamanna, F. Rogister, O. Deparis, P. Megret, M. Blondel, and T. Erneux, "Bifurcation to polarization self-modulation in vertical-cavity surface-emitting lasers," Opt. Lett. **27**, 261–263 (2002).
25. S. Kakuma and R. Ohba, "Practical accurate optical ranging based on polarization self modulation of a vertical-cavity surface-emitting laser diode," Opt. Rev. **10**, 511–513 (2003).
26. J. Javaloyes, J. Mulet, and S. Balle, "Passive mode locking of lasers by crossed-polarization gain modulation," Phys. Rev. Lett. **97**, 163902 (2006).
27. W. L. Zhang, W. Pan, B. Luo, X. H. Zou, and M. Y. Wang, "Polarization dynamics of vertical-cavity surface-emitting lasers with optical feedback," Opt. Eng. (Bellingham) **45**, 114202 (2006).